2024 IEEE/RSJ International Conference on Intelligent Robots and Systems (IROS)
October 14-18, 2024. Abu Dhabi, UAE

Using Hip Assisted Running Exoskeleton with Impact Isolation Mechanism to Improve Energy Efficiency

Ziqi Wang[1], Junchen Liu[1], Hongwu Li[1], Qinghua Zhang[1], Xianglong Li[1], Yi Huang[1], Haotian Ju[1], Tianjiao Zheng[1], Jie Zhao[1] *Member, IEEE*, and Yanhe Zhu*[1], *Member, IEEE*

***Abstract*— Research has indicated that exoskeletons can assist human movement, but due to the influence of additional weight and challenges in control strategy design, only a few exoskeletons effectively reduce the wearers' metabolic costs during running. This paper proposes an innovative and efficient hip-assisted running exoskeleton (HARE) designed to facilitate the flexion and extension movements of the joint along the sagittal plane. In the field of structural engineering, we propose implementing an active-passive combination constant force suspension system, hereinafter referred to as CFS, to effectively mitigate the impact of inertial forces during running. The decoupled transmission mechanism allows the CFS and assist mechanisms to operate independently, ensuring the tension of the cables. The flexible structural design can reduce the locomotion limitation on human bodies and reduce the additional energy burden on the body. In control strategy designing, the joint torque-generating strategy provides personalized assistance strategies for wearers to actively optimize the control parameters. Meanwhile, the safety control strategy based on abnormal gait recognition can ensure human safety. Experiments have shown that compared to not wearing exoskeletons, this device can reduce the energy consumption of the human body by 5.33 % at a speed of 9 km/h. This demonstrates its potential in human motion assistance processes.**

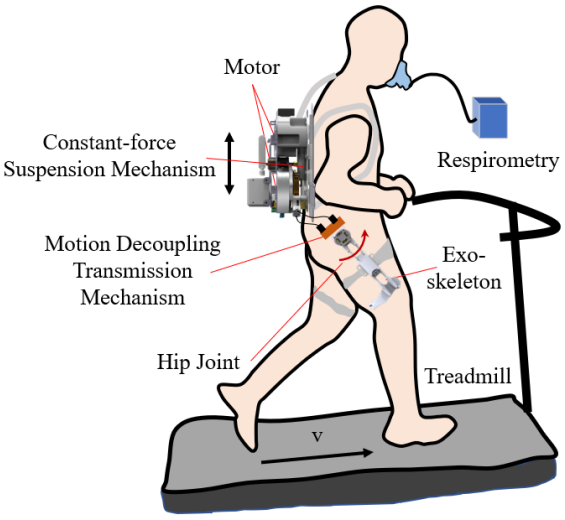

Fig. 1. Concept diagram of metabolic cost testing during running wearing HARE. The joint drive torque is transmitted from the constant force suspension mechanism on the back to the motion decoupling transmission mechanism and ultimately acts on the hip joint.

I. INTRODUCTION

Running can reduce the risk of certain chronic diseases and alleviate anxiety and depression [1]–[7]. Exoskeletons used as running assists may increase participation in running, helping maintain a healthy physique and enhancing their sense of participation, achievement and happiness [8]. However, while hip joint-assisted exoskeletons have been proven to have an assisting effect in daily exercise and labor scenarios [9], only a few can significantly reduce energy consumption during running. The reasons can be divided into the following points:

Firstly, changes in the quality and distribution of human-machine systems can have an impact on the normal rhythmic movement of the human body [10]. Due to the fact that the weight of the load carried by the human body is directly proportional to the amount of metabolism [11]–[13], lightweight exoskeletons help to avoid additional energy consumption. A group of representatives have emerged in this area in recent years [14]–[17]. Research has shown that mass located away from the center of gravity during running significantly increases the wearer's metabolic cost [10], [18]. It can also reduce the comfort of the device wearer [19] and even affects the user's level of technical acceptance [20]. Therefore, although the proportion of energy consumption during running is relatively small [21], hip joint assisted exoskeletons with relatively small arm lengths are still a promising assistive device. In addition, unloading additional mass onto the ground is a possible technical route, but additional constraints on the human body may have a negative impact on subjective perception and objective metabolic costs. Flexible exoskeleton clothing can comfortably transmit torque to users, but it can lead to a loss of peak torque [22].

Secondly, additional mass during exercise can generate inertial forces on the human body, which may be a source of metabolic load and musculoskeletal damage [23], [24]. A CFS system that can isolate inertial impacts is an effective means of coping. Previous studies have shown that carrying elastic suspension loads can improve the biomechanical performance of the human body and reduce its burden compared to carrying rigid loads [25]. The current theory has confirmed the possibility of using purely passive means to achieve

This work was supported by the National Outstanding Youth Science Fund Project of China under Grant 52025054 and the National Natural Science Foundation of China under Grant 52105016.(Corresponding author: Yanhe Zhu.)*

This work involved human subjects in its research. Approval of all ethical and experimental procedures and protocols was granted by the Medical Ethics Committee of Harbin Institute of Technology, China, ethics number HIT-2023052.

[1]The authors are with the State Key Laboratory of Robotics and Systems, Harbin Institute of Technology, Harbin 150080, China

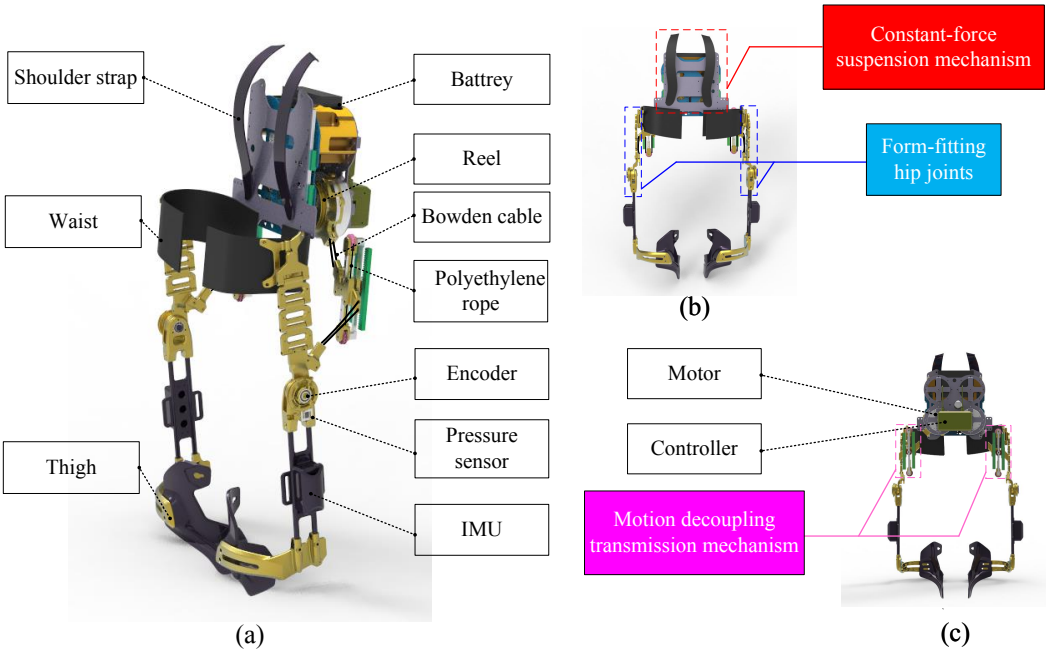

Fig. 2. Overview of HARE. HARE consists of three parts: constant force suspension mechanism, motion decoupling transmission mechanism and form-fitting hip joints. HARE weighs 5.5 kg, includes two drives and one battery, and can last for 2 hours while walking. The exoskeleton has two activated degrees of freedom, including flexion and extension of two hip joints. The maximum torque and angular velocity of hip flexion and extension is 18 N·m (226 r/min).

inertial impact isolation [26], but it is difficult to achieve in practice due to sensor errors and mechanical structure friction. This requires an active control method that can compensate for inertial forces. The current methods include active stiffness adjustment of suspended mechanism [27], acceleration control based on disturbance observers [28], and pump TENG technology (PBP-TENG) [29], but these methods are mainly used to improve walking economy and lack validation under running conditions.

Thirdly, assistance in high-speed motion requires a more rapid and accurate control strategy. The human body can withstand 5% torque variability while walking [30], however, the range of motion of the center of mass increases and the stability decreases while running, requiring faster recognition of gait phase and more robust application of joint torque. Previous studies have confirmed the benefits of personalized assistance in assisting human movement. Human-in-the-Loop optimization [31], [32] and preference based optimization [33], [34] methods are two paradigms in this field, and have achieved good results. However, these methods lack anomaly detection measures during high-speed human movement, and new personalized safety assistance strategies need to be studied for running assistance scenarios.

In order to achieve running assistance, we developed a flexible autonomous hip assisted running exoskeleton called HARE, which does not interfere with human movement based on our existing work [26]. Fig. 1 conceptually shows our proposed running assisted exoskeleton system. Fig. 2 reveals the complete design of HARE. This device can utilize a CFS mechanism that combines active and passive forces to isolate impacts and achieve ground suspension of loads. The independent operation between the CFS mechanism and the exoskeleton joint assistance mechanism is achieved through a motion decoupled transmission mechanism. And by detecting conflicts between the exoskeleton and the human body, running assistance can be achieved while ensuring safety. The preliminary experimental results demonstrate its hope in reducing metabolic cost and ensuring exercise safety.

The subsequent sections are organized as follows: Section II primarily presents the system structure design of HARE. Section III outlines the experiments and corresponding results. Eventually, Section IV provides conclusion and discussion.

II. DESIGN OF HARE

A. Previous work

Our previous generation of motion-assisted lower limb exoskeletons featured a passive CFS mechanism, which provided walking and running assistance through combined hip and knee joint support. During the experiment, it was found that heavy weight of this exoskeleton led to adverse effects on metabolic cost.Moreover, excessive constraints between the device and the human body not only affect user comfort and subjective experience, but also fail to bring significant improvements to the energy efficiency of the human body. Compared to normal walking, the shaking amplitude of the center of mass during human running increases, and the back is usually unable to maintain parallelism with the direction of gravity, resulting in a decrease in the suspension effect of the CFS mechanism. The joint assistance of exoskeletons

can also have a negative impact on the suspension effect of CFS mechanism, ultimately leading to some users not being able to reduce their metabolism with the use of the CFS mechanism. Moreover, this device is not specifically designed for running assistance and lacks considerations for personalized joint torque curves and motion assistance safety.

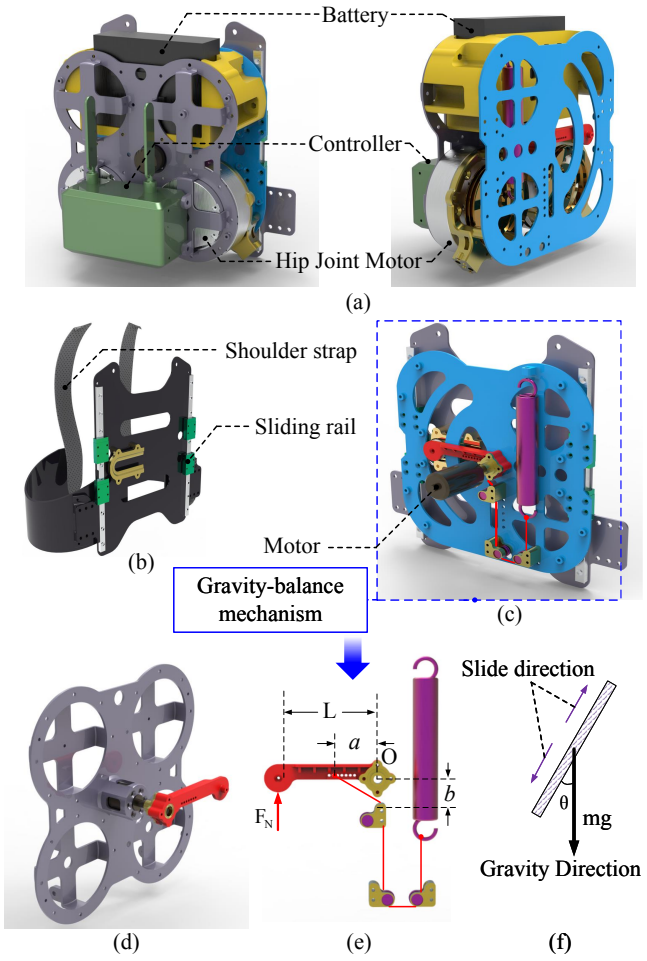

Fig. 3. Components and structural principles of the constant force suspension mechanism. (a) Picture of the constant force suspension mechanism and additional components. (b) Stationary components of the constant force suspension mechanism. (c) The active passive combined gravity balance system is a floating component of a constant force suspension mechanism. (d) Installation position of active motor in floating mechanism. (e) Principle of the gravity-balance mechanism. (f) Gravity balance of a constant force suspension mechanism when tilted.

B. Design of constant force suspension mechanism

1) Structural design of constant force suspension mechanism: As illustrated in Fig. 3, the CFS mechanism consists of a swing arm, wire rope, motor, coupling and spring. One extremity of the swing arm is pivotally attached on the floating component, while the other extremity is linked to the horizontal slide rail via a sliding pair. The gravity on the floating component can be transmitted to the stationary component via horizontal sliding rails.. The motor drives the swing arm via the coupling, while the spring is operated by the wire rope. As the individual moves, the swing arm undergoes rotation in conjunction with the vertical displacement of the floating element, causing the wire rope to adjust the spring's elongation synchronously.

As shown in Fig. 3(d), a Robomaster M2006 brushless DC motor is installed at the rotation center of the swing arm to achieve active control of the CFS mechanism. The maximum torque of the motor is 1 N.m and the mass is 95g. The lightweight motor can reduce the impact of additional mass on the suspension effect while providing active control torque.

2) Mathematical modeling of constant force suspension mechanism: According to reference [26], when the overall potential energy of the system remains constant, the equation in the CFS mechanism is:

$$mgL = kab \tag{1}$$

where the variables m, g and k represent the mass of the floating component, the acceleration due to gravity, and the stiffness of the spring, respectively; a and b are the constants related to structure, marked in Fig. 3 (e).

When the direction of the CFS mechanism guide rail is not collinear with the direction of gravity, as shown in Fig. 3(f), this equation becomes:

$$mgLcos\theta = kfab \tag{2}$$

where θ is the angle between two directions, f is the ratio of k changes in this situation.

To compensate for changes in the stiffness of the original spring, the motor is used as a virtual negative stiffness spring:

$$mgLcos\theta = (k + k_m)ab \tag{3}$$

where k_m is the negative stiffness of motor compensation.

3) Fuzzy control strategy for constant force suspension mechanism: In practice, mechanical systems are affected by nonlinear friction, which can weaken the suspension effect of the CFS mechanism. In addition, the variation of the guide wheel wrap angle with position in the CFS mechanism may lead to changes in constants a and b. Currently, experiments have proven the nonlinearity of this CFS mechanism. Fuzzy PID control method does not depend on an exact mathematical model of the system and offers benefits in addressing control challenges associated with nonlinear systems. Therefore, using fuzzy PID control to compensate for the stiffness metric k_m in the motor compensation Eq. 3.

C. Hip joint assisted exoskeleton design

1) Design of flexible hip joint mechanism: To minimize the adverse effects of distal mass on human metabolism, sagittal flexion/extension of the hip joint is chosen as the sole assisted joint. Hip joint exercise accounts for 32-39% of total energy consumption during running [35]. Although the motion assistance of a single joint in other planes has been proven to have positive benefits for energy economy and stability [36], it can avoid the adverse effects of confinement on metabolic cost and further reduce overall mass.

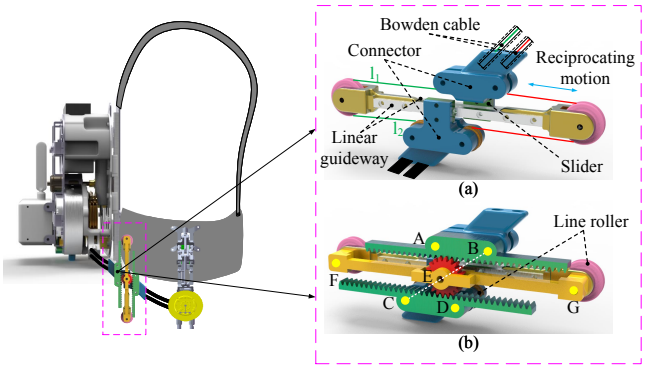

Fig. 4. Design of motion decoupling transmission mechanism. (a) The components of the decoupling transmission mechanism and the winding method of Bowden cable in motion decoupling transmission mechanism. (b) Schematic diagram of the working principle of motion decoupling transmission mechanism.

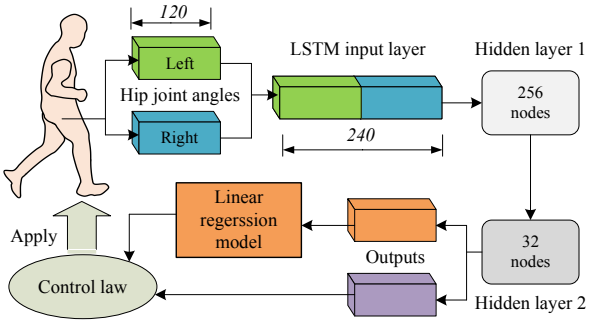

Fig. 5. The method of gait percentage predict. LSTM determines the historical data sequence of left and right hip joint angles, outputs gait percentage and abnormal gait classification. The percentage of gait is linearized by the linear regression model and applied to torque control.

HARE's hip joint adopts a hinged design, with the waist connector controlling rotation and the hinge controlling yaw. The line wheel at the end of the hinge is connected to the Bowden cable to facilitate the movement of flexion and extension in the hip joint.

2) Design of transmission mechanism decoupled from constant force suspension mechanism: The Bowden cable may be forced to bend during the up-and-down movement of the CFS mechanism, resulting in nonlinear and time-varying elastic interference with the balance of the CFS mechanism. This is undoubtedly an urgent problem that needs to be solved.

The transmission mechanism used for decoupling is shown in Fig 4. This decoupling transmission mechanism can be divided into three parts: connecting components between upper and lower levels, and a fixed pulley group in the middle. There are two guide wheels installed on the connector, located at positions A, B, and C, D. There is a gear at the intersection point E between the fixed pulley group and the opposite guide wheels B and C of the connecting parts, which can mesh with the racks on both sides of the connecting parts. The reversing effect of gears causes the movement direction of the connecting parts on both sides to be opposite.

The wrapped cable passes through guide wheel C to fixed pulley F, and then returns to the Bowden cable through guide wheel A, with the opposite side cable arranged in mirror symmetry. Due to the mirror symmetry of the movement of the connecting parts on both sides of the gear, the sum of the changes in cable length CF and AF is always 0. Therefore, the up and down movement of the connector on the other side will not affect the overall length of the cable. The motion on both sides of the transmission mechanism is independent of each other, achieving motion decoupling between the CFS mechanism and the joint assist mechanism.

3) Gait percentage recognition and anomaly detection: In order to make the applied joint torque conform to the rhythmic movement of the human body, it is necessary to apply joint torque according to the percentage of human gait, so a fast and accurate gait estimation model is needed. The gait estimation model utilizes a multi-layer neural network architecture that is founded on long short-term memory. Its input data type is the Euler angle of hip joint bending and extension, with a time series length of 120; The output dimension is 2, which includes gait percentage and abnormal gait classification information. This model has 2 hidden layers with 256 and 32 nodes, respectively. The process of predicting gait percentage through artificial neural networks is shown in Fig. 5.

Collect joint angle data of human motion at speeds of 3, 5, 7, and 9 km/h on a treadmill for training neural networks. Move the left hip joint forward to its maximum position to determine the beginning and end of a gait cycle, and manually label the gait percentage. The negative samples contain abnormal movement states such as squatting, bouncing, and side kicking, and the data is augmented by adding Gaussian noise.

The output of neural networks usually has small fluctuations, which can lead to unstable joint torque output and have adverse effects on human perception. To avoid this issue, a linear regression model is used to linearize the output of the neural network. The linear regression model can calculate the average gradient of gait percentage over a period of time and perform regression according to Eq. 4:

$$\hat{x} = \overline{k}\Delta t \tag{4}$$

Where $\hat{x}$ is the final estimated value of the gait percentage, $\overline{k}$ is the average gradient calculated by the least square method during the sliding time window Δt.

4) Personalized User-Defined assistance for Hip Joint During Running: Personalized assistance strategies (e.g. HIL [37]) could provide targeted assistance for the wearers during locomotion and have been paid more and more attention in recent years. These methods usually optimize the control parameters according to the wearers' personalized gaits, energy consumption feedback, preferences, and so on. This allows this personalized approach to provide the most appropriate auxiliary strategy for each wearer and maximize the actual

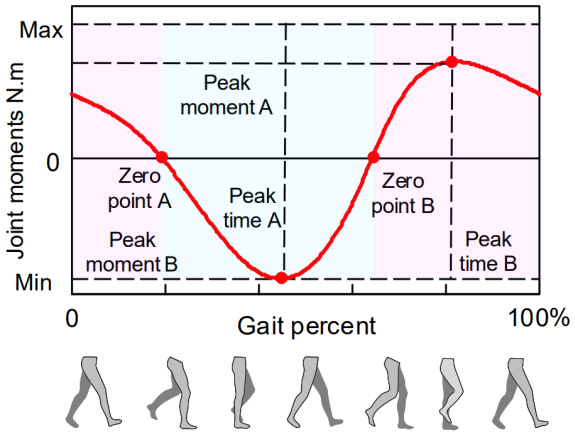

Fig. 6. Diagram of personalized joint torque generation process. Wearers can explore personalized joint curve torque by adjusting the zero and peak points in the graph.

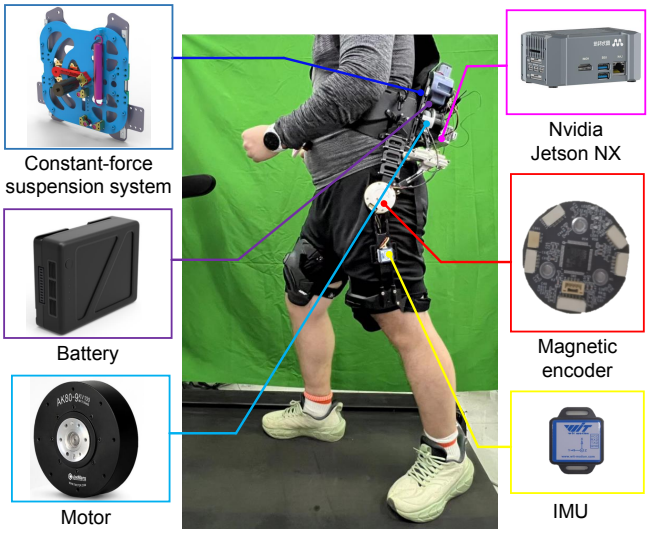

Fig. 7. Experimental Platform. The main information of the exoskeleton is listed as follows: constant force suspension system, battery (TB50, DJI, China), gear motor (AK80-9, Cubemars, China), inertial measurement unit (IMU) (WT61C, WIT, China), self-designed encoder and CAN master board, and embedded computer (Jetson NX, Nvidia, USA).

assistive effect.

In this work, we proposed a personalized user-defined optimized method for the wearers, which allows the wearers to actively manually tune the hip joint moments according to their subjective feelings about the assistance performance. As shown in Fig. 6, the joint moments of the hip joints are predefined as a sinusoidal curve. The shape of the curves is ensured according to two peak moment points and two zero points. During the tuning process, the wearers are able to manually adjust the joint moment curves by tuning the coordinates of these key points. The subjective feelings about assistance performance, the comprehension and cognition of the control parameters, and the feeling of comfort will guide the wearer during the adjustment process. During the process of running, the external forces on human bodies can easily lead to serious consequences such as falling. To avoid these risks, the gait prediction model described in II-C.3 can also recognize whether there is an abnormal gait. When an abnormal gait occurs, the aim joint moments are set as 0 N.m to maintain the stability and balance of subjects.

III. EXPERIMENTS AND RESULTS

This section evaluates the performance of the HARE when applied to running. The proposed wearable device and its main mechanism are shown in Fig. 7.

A. constant force suspension system effect evaluation

In order to verify the effectiveness of the CFS mechanism, we conducted a series of experiments to verify the isolation capability of the force of impact. The force of impact exerted by the floating component on the human body can be calculated by detecting its acceleration. As shown in Fig. 8, in different speed experiments, the acceleration obtained by the floating component test has significantly decreased, which verifies that the mechanism designed by us has the capability to substantially diminish the impact force produced during human motion.

B. Personalized joint torque adjustment for different subjects

Volunteers dynamically adjusted the torque values at key points in the gait cycle based on their perceived assistance before and after different states, then fitted the final spline curve.The joint torque curve results of different subjects are shown in Fig. 9.

C. Metabolic cost

To assess the true impact of the suggested design of the wearable device structure and verify the actual use effect, the metabolic expenditure of individuals wearing the items

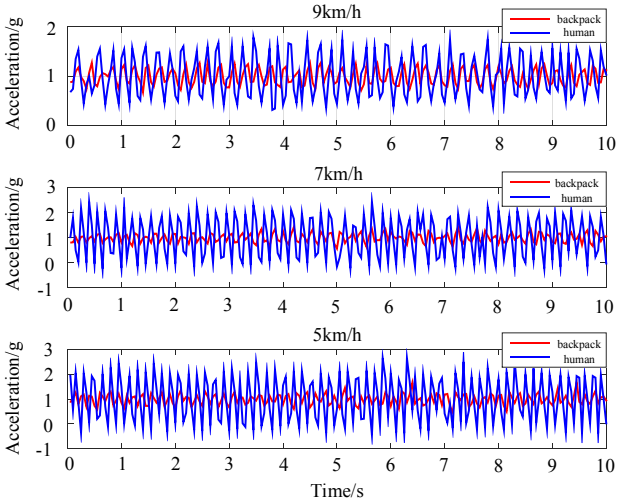

Fig. 8. The floating effect of the constant force suspension system in different velocities.

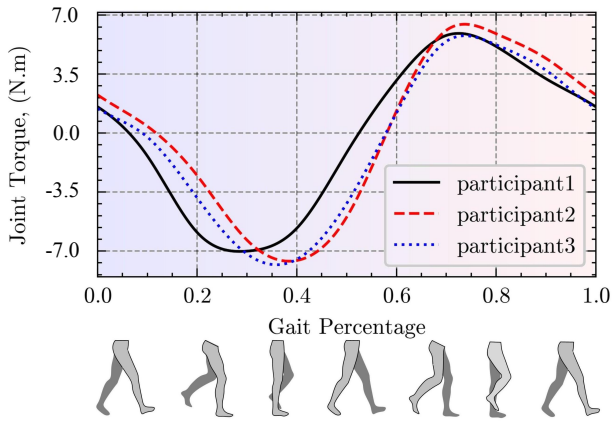

Fig. 9. Personalized joint torque curve results of different individuals.

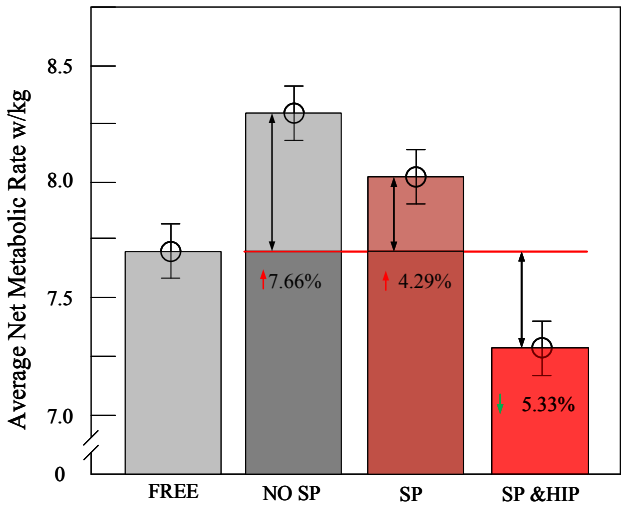

Fig. 10. Average metabolic cost of six subjects under FREE, NO SP, SP, and SP & HIP conditions at the speed of 9 km/h.

running on a treadmill at a speed of 9 km/h was quantified. The upper torque limit is set to the rated torque of the motor, which is 9 N.m.

We selected 6 healthy experimental participants (age: 27.0 ± 3.0 years; height: 1.77 ± 0.03 m; weight: 80.5 ± 15.5 kg).To evaluate the effect of the suspension mechanism, we measured the energy consumption in four different scenarios: Free, No SP, SP, SP&HIP, where Free means that the subject refrained from utilizing the suspension apparatus throughout the duration of the experiment. No SP means that the CFS mechanism was used locked, the floating component was mounted directly on its back to eliminate the influence of the weight of the suspension mechanism on the test results. SP indicates that the suspension mechanism is on. SP&HIP is the ultimate experimental condition for testers will be protected by the back suspension mechanism and assisted by the hip joint torque at the same time. For each state, measurements were conducted using a portable metabolic system (K5, COSMED, Italy for the purpose of recording oxygen consumption and carbon dioxide production. The experimental procedure is delineated as follows:

1) In order to eliminate the impact of the tester's physiological fatigue on the experimental data as much as possible and ensure the independence between each set of data, we chose to conduct four sets of tests in the same time interval for four consecutive days.

2) Before running, the wearer should stand still for 3 minutes to ensure stable breathing.

3) The wearers run on a treadmill at a speed of 9 km/h and a 0 degree slope for 4 minutes to ensure that the intake of oxygen and carbon dioxide remains relatively stable.

4) After running, the wearer should stand still for 3 minutes and wait for breathing to stabilize.

We use the modified Brockway equation [38] to calculate the power consumption per kilogram of energy, and the results are shown in Fig. 10. By comparing the four sets of experimental results, we can discover some valuable information.

Experimental results show that the design achieves the expected goals of weakening motion interference and reducing impact force. At a speed of 9 km/h, compared with the FREE condition, the average net metabolism of the participant wearing proposed device in the No SP and SP increased by 7.66 % and 4.29 % respectively, indicating that the wearable device can effectively help the wearers reduce metabolic costs caused by inertial force impact while running. In the SP&HIP state, the average oxygen consumption of testers was significantly reduced by 5.33 %, indicating that this set of equipment has the function of effectively assisting human running.

IV. CONCLUSION AND DISCUSSION

In this article, building on our previous walking exoskeleton, we proposed a wearable device for running with a self-regulating CFS mechanism, expanding its application scenarios. This research can be succinctly outlined as follows. Primarily, the CFS mechanism designed can reduce the impact force generated during the running process of the human body at different speeds obviously. Secondly, in the case of high-speed running, experimental results prove that wearing this device significantly reduces metabolic costs. In addition,control strategies based on abnormal gait recognition can effectively ensure the safety of human running processes, which can make certain contributions to human body rehabilitation training and sports enhancement in the post-COVID-19 era. Finally,this set of device is also expected to serve as a universal exoskeleton platform for integrating motors, batteries, and other inertial impact components, and may be adopted by various research teams for different lower limb exoskeletons.

However, there are still several shortcomings in our work which should be improved. We need to increase the length of the guide rail to accommodate substantial changes in the center of mass, and conduct multiple sets of tests on more individuals at greater speeds to evaluate the effect of the system operating more objectively at different speeds.

REFERENCES

[1] W. H. Organization, *Global health risks: mortality and burden of disease attributable to selected major risks*. World Health Organization, 2009.

[2] D.-c. Lee, A. G. Brellenthin, P. D. Thompson, X. Sui, I.-M. Lee, and C. J. Lavie, "Running as a key lifestyle medicine for longevity," *Progress in cardiovascular diseases*, vol. 60, no. 1, pp. 45–55, 2017.

[3] Z. Pedisic, N. Shrestha, S. Kovalchik, E. Stamatakis, N. Liangruenrom, J. Grgic, S. Titze, S. J. Biddle, A. E. Bauman, and P. Oja, "Is running associated with a lower risk of all-cause, cardiovascular and cancer mortality, and is the more the better? a systematic review and meta-analysis," *British journal of sports medicine*, vol. 54, no. 15, pp. 898–905, 2020.

[4] D.-c. Lee, R. R. Pate, C. J. Lavie, X. Sui, T. S. Church, and S. N. Blair, "Leisure-time running reduces all-cause and cardiovascular mortality risk," *Journal of the American College of Cardiology*, vol. 64, no. 5, pp. 472–481, 2014.

[5] E. J. Doyne, D. J. Ossip-Klein, E. D. Bowman, K. M. Osborn, I. B. McDougall-Wilson, and R. A. Neimeyer, "Running versus weight lifting in the treatment of depression." *Journal of consulting and clinical psychology*, vol. 55, no. 5, p. 748, 1987.

[6] S. A. Paluska and T. L. Schwenk, "Physical activity and mental health: current concepts," *Sports medicine*, vol. 29, pp. 167–180, 2000.

[7] C. R. Richardson, G. Faulkner, J. McDevitt, G. S. Skrinar, D. S. Hutchinson, and J. D. Piette, "Integrating physical activity into mental health services for persons with serious mental illness," *Psychiatric services*, vol. 56, no. 3, pp. 324–331, 2005.

[8] H.-J. F. Zunft, D. Friebe, B. Seppelt, K. Widhalm, A.-M. R. de Winter, M. D. V. de Almeida, J. M. Kearney, and M. Gibney, "Perceived benefits and barriers to physical activity in a nationally representative sample in the european union," *Public health nutrition*, vol. 2, no. 1a, pp. 153–160, 1999.

[9] C. Siviy, L. M. Baker, B. T. Quinlivan, F. Porciuncula, K. Swaminathan, L. N. Awad, and C. J. Walsh, "Opportunities and challenges in the development of exoskeletons for locomotor assistance," *Nature Biomedical Engineering*, vol. 7, no. 4, pp. 456–472, 2023.

[10] J. Kim, G. Lee, R. Heimgartner, D. Arumukhom Revi, N. Karavas, D. Nathanson, I. Galiana, A. Eckert-Erdheim, P. Murphy, D. Perry *et al.*, "Reducing the metabolic rate of walking and running with a versatile, portable exosuit," *Science*, vol. 365, no. 6454, pp. 668–672, 2019.

[11] T. M. Griffin, T. J. Roberts, and R. Kram, "Metabolic cost of generating muscular force in human walking: insights from load-carrying and speed experiments," *Journal of applied physiology*, vol. 95, no. 1, pp. 172–183, 2003.

[12] G. J. Bastien, P. A. Willems, B. Schepens, and N. C. Heglund, "Effect of load and speed on the energetic cost of human walking," *European journal of applied physiology*, vol. 94, pp. 76–83, 2005.

[13] A. Grabowski, C. T. Farley, and R. Kram, "Independent metabolic costs of supporting body weight and accelerating body mass during walking," *Journal of applied physiology*, vol. 98, no. 2, pp. 579–583, 2005.

[14] G. Lee, J. Kim, F. Panizzolo, Y. Zhou, L. Baker, I. Galiana, P. Malcolm, and C. Walsh, "Reducing the metabolic cost of running with a tethered soft exosuit," *Science Robotics*, vol. 2, no. 6, p. eaan6708, 2017.

[15] R. Nasiri, A. Ahmadi, and M. N. Ahmadabadi, "Reducing the energy cost of human running using an unpowered exoskeleton," *IEEE Transactions on Neural Systems and Rehabilitation Engineering*, vol. 26, no. 10, pp. 2026–2032, 2018.

[16] J. Kim, R. Heimgartner, G. Lee, N. Karavas, D. Perry, D. L. Ryan, A. Eckert-Erdheim, P. Murphy, D. K. Choe, I. Galiana *et al.*, "Autonomous and portable soft exosuit for hip extension assistance with online walking and running detection algorithm," in *2018 IEEE International Conference on Robotics and Automation (ICRA)*. IEEE, 2018, pp. 5473–5480.

[17] C. S. Simpson, C. G. Welker, S. D. Uhlrich, S. M. Sketch, R. W. Jackson, S. L. Delp, S. H. Collins, J. C. Selinger, and E. W. Hawkes, "Connecting the legs with a spring improves human running economy," *Journal of Experimental Biology*, vol. 222, no. 17, p. jeb202895, 2019.

[18] R. C. Browning, J. R. Modica, R. Kram, and A. Goswami, "The effects of adding mass to the legs on the energetics and biomechanics of walking," *Medicine & Science in Sports & Exercise*, vol. 39, no. 3, pp. 515–525, 2007.

[19] K. A. Ingraham, M. Tucker, A. D. Ames, E. J. Rouse, and M. K. Shepherd, "Leveraging user preference in the design and evaluation of lower-limb exoskeletons and prostheses," *Current Opinion in Biomedical Engineering*, p. 100487, 2023.

[20] F. D. Davis, "Perceived usefulness, perceived ease of use, and user acceptance of information technology," *MIS quarterly*, pp. 319–340, 1989.

[21] A. Belli, H. Kyröläinen, and P. Komi, "Moment and power of lower limb joints in running," *International journal of sports medicine*, vol. 23, no. 02, pp. 136–141, 2002.

[22] D. E. Miller, G. R. Tan, E. M. Farina, A. L. Sheets-Singer, and S. H. Collins, "Characterizing the relationship between peak assistance torque and metabolic cost reduction during running with ankle exoskeletons," *Journal of neuroengineering and rehabilitation*, vol. 19, no. 1, p. 46, 2022.

[23] L. C. Rome, L. Flynn, and T. D. Yoo, "Rubber bands reduce the cost of carrying loads," *Nature*, vol. 444, no. 7122, pp. 1023–1024, 2006.

[24] L. Huang, Z. Yang, R. Wang, and L. Xie, "Physiological and biomechanical effects on the human musculoskeletal system while carrying a suspended-load backpack," *Journal of Biomechanics*, vol. 108, p. 109894, 2020.

[25] Y. Leng, X. Lin, R. Deng, J. Chang, L. Yang, K. Zhang, and C. Fu, "Design and implement an elastically suspended back frame for reducing the burden of carrier," in *2021 6th IEEE International Conference on Advanced Robotics and Mechatronics (ICARM)*. IEEE, 2021, pp. 236–240.

[26] H. Li, D. Sui, H. Ju, Y. An, J. Zhao, and Y. Zhu, "Mechanical compliance and dynamic load isolation design of lower limb exoskeleton for locomotion assistance," *IEEE/ASME Transactions on Mechatronics*, vol. 27, no. 6, pp. 5392–5402, 2022.

[27] Y. Leng, X. Lin, L. Yang, Y. Xu, and C. Fu, "Design of an elastically suspended backpack with tunable stiffness," in *2020 5th International Conference on Advanced Robotics and Mechatronics (ICARM)*. IEEE, 2020, pp. 359–363.

[28] L. He, C. Xiong, Q. Zhang, W. Chen, C. Fu, and K.-M. Lee, "A backpack minimizing the vertical acceleration of the load improves the economy of human walking," *IEEE Transactions on Neural Systems and Rehabilitation Engineering*, vol. 28, no. 9, pp. 1994–2004, 2020.

[29] Z. Yang, Y. Yang, J. Shen, A. Li, X. Qu, Z. Lai, L. Ji, J. Chen, and J. Cheng, "Load-suspended power backpack for labor saving and energy harvesting from human walk," *Nano Energy*, vol. 121, p. 109190, 2024.

[30] M. I. Wu and L. Stirling, "Impact of imperfect exoskeleton algorithms on step characteristics, task performance, and perception of exoskeleton performance," in *2023 IEEE/RSJ International Conference on Intelligent Robots and Systems (IROS)*. IEEE, 2023, pp. 4088–4093.

[31] J. Zhang, P. Fiers, K. A. Witte, R. W. Jackson, K. L. Poggensee, C. G. Atkeson, and S. H. Collins, "Human-in-the-loop optimization of exoskeleton assistance during walking," *Science*, vol. 356, no. 6344, pp. 1280–1284, 2017.

[32] Y. Ding, M. Kim, S. Kuindersma, and C. J. Walsh, "Human-in-the-loop optimization of hip assistance with a soft exosuit during walking," *Science robotics*, vol. 3, no. 15, p. eaar5438, 2018.

[33] M. Tucker, M. Cheng, E. Novoseller, R. Cheng, Y. Yue, J. W. Burdick, and A. D. Ames, "Human preference-based learning for high-dimensional optimization of exoskeleton walking gaits," in *2020 IEEE/RSJ International Conference on Intelligent Robots and Systems (IROS)*. IEEE, 2020, pp. 3423–3430.

[34] K. A. Ingraham, C. D. Remy, and E. J. Rouse, "The role of user preference in the customized control of robotic exoskeletons," *Science robotics*, vol. 7, no. 64, p. eabj3487, 2022.

[35] D. J. Farris and G. S. Sawicki, "The mechanics and energetics of human walking and running: a joint level perspective," *Journal of The Royal Society Interface*, vol. 9, no. 66, pp. 110–118, 2012.

[36] J. Park, K. Nam, J. Yun, J. Moon, J. Ryu, S. Park, S. Yang, A. Nasirzadeh, W. Nam, S. Ramadurai *et al.*, "Effect of hip abduction assistance on metabolic cost and balance during human walking," *Science Robotics*, vol. 8, no. 83, p. eade0876, 2023.

[37] K. A. Witte, P. Fiers, A. L. Sheets-Singer, and S. H. Collins, "Improving the energy economy of human running with powered and unpowered ankle exoskeleton assistance," *Science Robotics*, vol. 5, no. 40, p. eaay9108, 2020.

[38] J. Brockway, "Derivation of formulae used to calculate energy expenditure in man." *Human nutrition. Clinical nutrition*, vol. 41, no. 6, pp. 463–471, 1987.